

PROCESS INDUCED DEFORMATION OF COMPOSITE MATERIALS: A STANDARDIZED L-SHAPE EXPERIMENTAL METHODOLOGY

Tao, G^{1*}, Reid, S², and Poursartip, A^{1,2}

¹ Department of Materials Engineering, The University of British Columbia, Vancouver, BC, Canada

² Convergent Manufacturing Technologies, Vancouver, BC, Canada

* Corresponding author (gavin@composites.ubc.ca)

Keywords: *process-induced deformation, spring-in, warpage*

ABSTRACT

The ability to consistently produce composite structures with controlled tolerances remains a challenge for the aerospace industry. On a smaller scale, L-shaped specimens are routinely used as representative geometries to study process-induced deformation (PID) for aerospace composite structures. However, uncertainties and variabilities in processing parameters, deformation definition and measurement procedure have made cross-comparison of datasets in the literature less meaningful than is desirable. If we are to successfully pool research and measurements of process induced deformation (PID) with high accuracy, it is necessary to have systematic and reproducible methods to analyze and report L-shape deformations.

In this paper, the conventional experimental method for studying and reporting L-shape deformation has been improved to address the variabilities in L-shape fabrication and measurement process. The methodology can accurately and automatically reduce laser CMM point cloud data, separating the L-shape deformation into corner spring-in and flange warpage components. Tooling characterization is also considered. The result is a framework which is capable of linking different processing parameters to specific manufacturing outcomes.

1 INTRODUCTION

Consistently producing parts with controlled tolerances remains a challenge in manufacturing composite structures. A representative geometry which captures the sources and mechanisms of process induced deformation is an L-shape. The residual stresses built up throughout the cure cycle cause a change in the L-shape's enclosed angle and the flatness of the flanges, commonly known as spring-in and warpage respectively Figure 1.

The combined number of specimens used to study process induced deformation in the reported literature is of the order of thousands. Although this may sound significant, it is a relatively small dataset given the importance of the problem. More importantly, when comparing L-shape results across different studies, the wide range of different processing parameters during manufacturing (sometimes unreported or implicit) makes comparison difficult. Variability during measuring and reporting L-shape geometry also add to the difficulties in comparing different PID datasets [1].

One often overlooked factor is tooling, which is often assumed to be perfect and reported L-shape spring-in angles are calculated based on the nominal tool angle. This will lead to inaccurate results if dimensional deviations or tool surface imperfections exist. Very few studies mentioned the measurement of tooling [2]–[7] and even fewer studies

have compensated the reported spring-in angles with actual tool angles (and which deviated from the nominal specification) [3], [7].

Currently, there is no standard or agreed-upon measurement method for determining L-shape deformation. Methods with various accuracy levels have been used in literature making it challenging to compare datasets across studies [1]. Currently, spring-in is commonly reported as a single value. Depending on whether the data was processed in 2D or 3D, a line (2D) or a plane (3D) is fitted to each flange of the specimen (Figure 1). Next, the L-shape angle is calculated from the normal of the lines or the planes. Then, the difference between the L-shape angle and the nominal angle is defined as the spring-in angle. When flange warpage is present, however, the result is dependent on the location of the fitted lines or planes as well as the flange length [8] (Figure 1b). Thus, a single spring-in angle value is insufficient to characterize L-shape distortion.

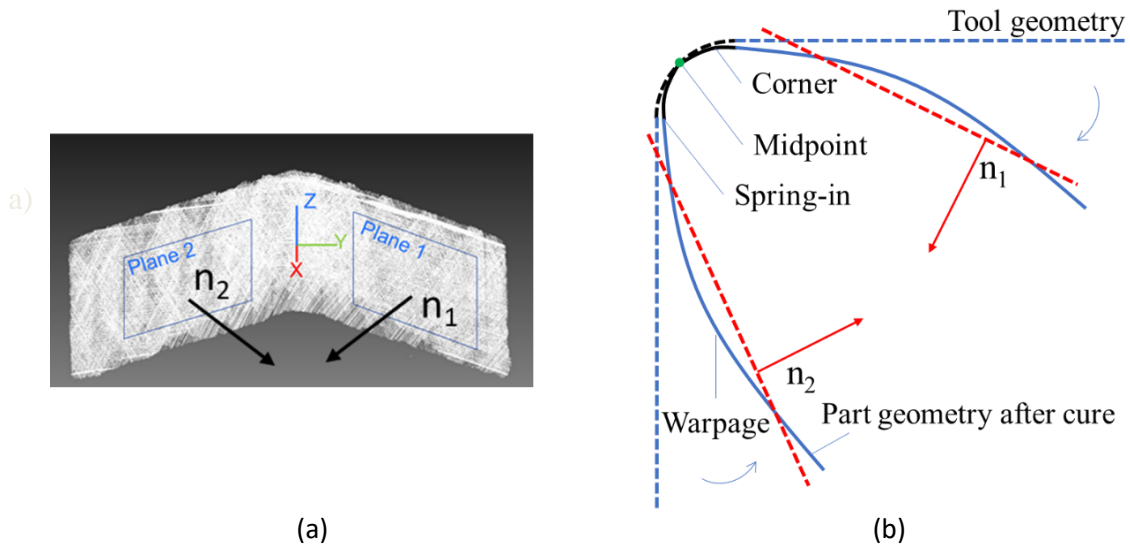


Figure 1 Traditional L-shape spring-in angle definition in (a) 3D and (b) 2D; it is insufficient to characterize deformation with a single spring-in value if flange warpage exists

This paper proposes a standardized L-shape experimental methodology in aiming to address the following variabilities found in literature:

- Inadequate spring-in definition
- Non-standardized reporting format
- Lack of tooling inspection and compensation
- Variation in measurement methods

2 Tooling evaluation

Tool thermal behavior and surface profile were first carefully evaluated. A robust data reduction process (implemented in Python) was then developed to measure and report the tool-compensated spring-in and warpage deformation separately. This methodology was demonstrated using a prepreg hand layup, autoclave cured L-shape which was then scanned using a Nikon Cera 7 laser coordinate measurement machine (CMM), aiming to specify what to measure and report, as well as standardizing the process for experimentally investigating PID.

Tool thermal behavior and surface profile should be characterized to quantify any deviation from the nominal dimensions. For illustration, an S-shaped invar tool's nominal tool dimensions and locations of interest are shown in

Figure 2. These locations were established by previous work to avoid non-uniform surface temperature during heat up caused by tooling substructures [9], [10].

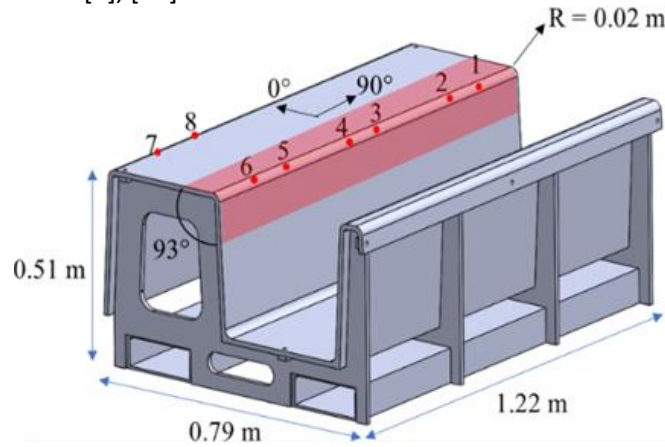


Figure 2 Invar tool dimensions and locations of interest. Areas with surface undulation is highlighted in red

Thermocouples were placed above the tool in the air as well as on the top and bottom surface at location 1, 2, 5 and 7. During a 2-hold cure cycle with a 5 °C/min rapid second ramp, the maximum temperature difference among locations 1, 2 and 5 was less than 2 °C. Location 7 lagged the other locations by about 2.5 °C due to poor airflow in the rear corner of the autoclave [10]. Consequently, location 7 was not used for fabricating specimens.

A FARO arm with 3 mm diameter ball probe was used to characterize the tool surface at room temperature. Upon initial inspection, although the tool surface meets a typical industrial geometrical dimensioning and tolerancing (GD&T) specifications for flatness (0.25 mm or 0.010 inch [11]), surface undulation were discovered. Undulations were most severe spanning from the corner outwards for 80 mm (

Figure 2). The average undulation over 80 mm for location 1 to 6 is 80 µm on the horizontal surface and 135 µm on the vertical surface. The effect of surface undulation on the tool angle can be estimated as:

$$\tan^{-1}\left(\frac{135 \times 10^{-6}}{80 \times 10^{-3}}\right) + \tan^{-1}\left(\frac{80 \times 10^{-6}}{80 \times 10^{-3}}\right) = 0.154^\circ$$

Thus for an L-shape part with an 80 mm flange length or shorter, the variation in tool angle at locations 1 to 6 is equivalent to a 0.15° error in reported spring-in if not accounted for.

3 Data reduction

A Python-based script was developed to reduce the point cloud data from the CMM and subsequently measure, then report the spring-in and warpage deformations. A flange length independent spring-in angle definition is incorporated into the script. Not only is the output compatible with existing results in the literature, it is also capable of characterizing L-shape local deformation, analyzing the spring-in and warpage separately.

The input of the script can be any types of 3D measurement in digital point cloud form (e.g. CMM, 3D scanner). For illustration this study uses the raw point cloud obtained by the CMM and the Nikon Focus Scan software. The script subsequently aligns, trims and slices the point cloud and detects the corner of the L-shapes (Figure 3). Then the L-shape slices are analyzed in 2D according to the steps in Table 1 to obtain the final spring-in plot. Steps g, h and i also included deviation plots to visualize the effect of flange warpage on the angle measurement. Note that the horizontal lines at deviation = 0 mm in steps g to i are the lines fitted during the corner/flange identification process. The angle between the two lines is not necessarily the nominal tool angle (here 93°).

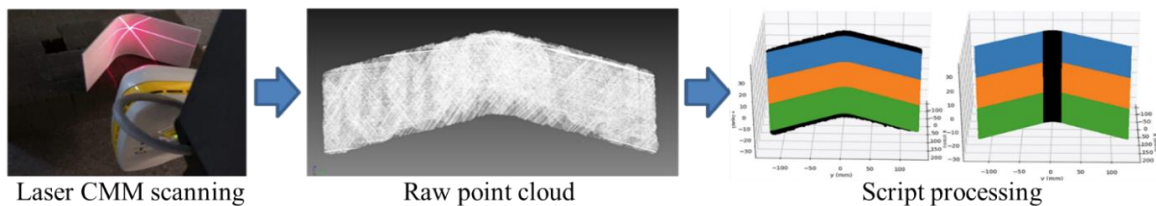


Figure 3 - 3D point cloud data obtained by Laser CMM scanning is input into the script where trimming, aligning and sectioning are performed. The corner section is also detected

The above analysis process is repeated for each slice of the L-shape point cloud and then averaged to generate an uncompensated spring-in plot. A typical uncompensated spring-in plot is shown in Figure 4b. The vertical axis is the angle formed by pairs of vectors subtracted by the nominal tool angle. The horizontal axis is the distance along the flanges of which the vectors are extended along. Each data point represents an angle measurement at a certain distance. The error bars represent the standard deviation of the three averaged slices.

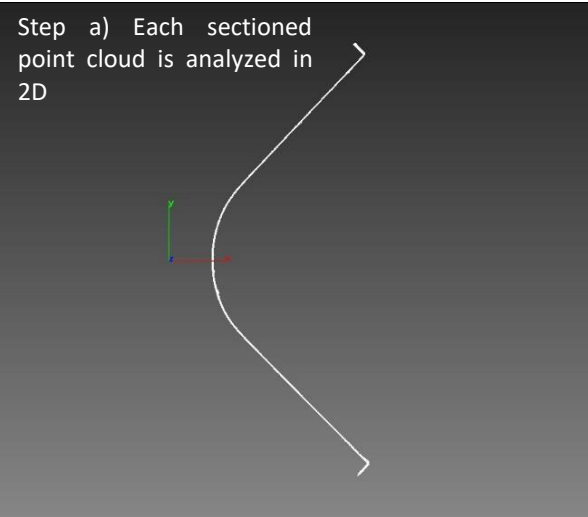
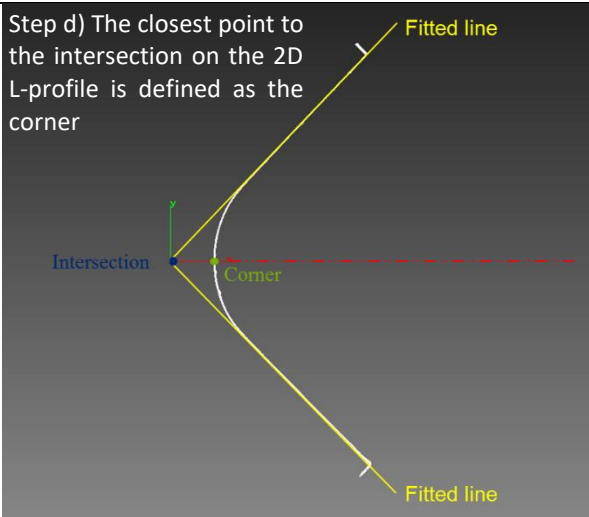
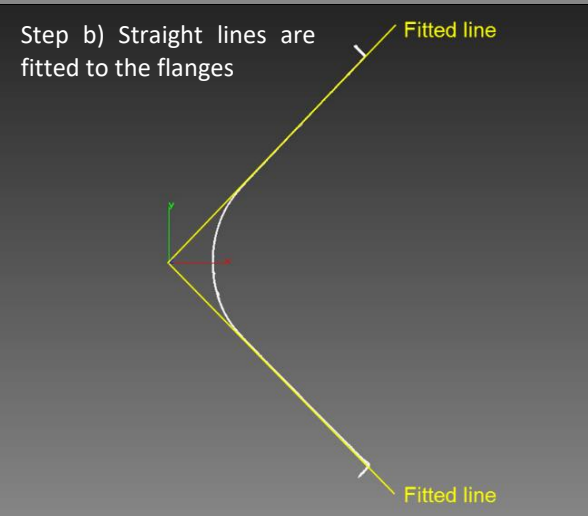
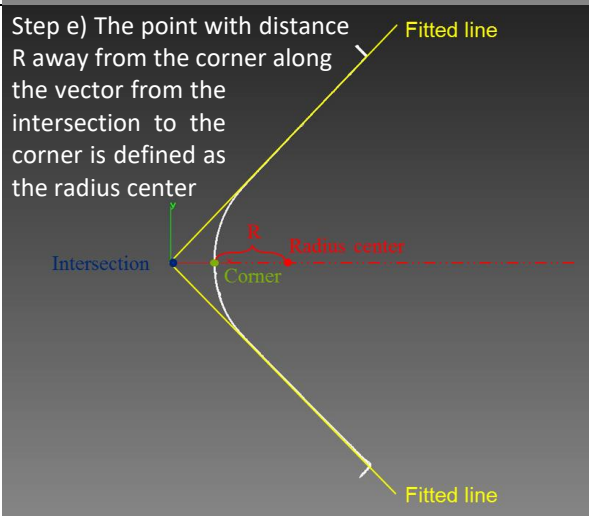
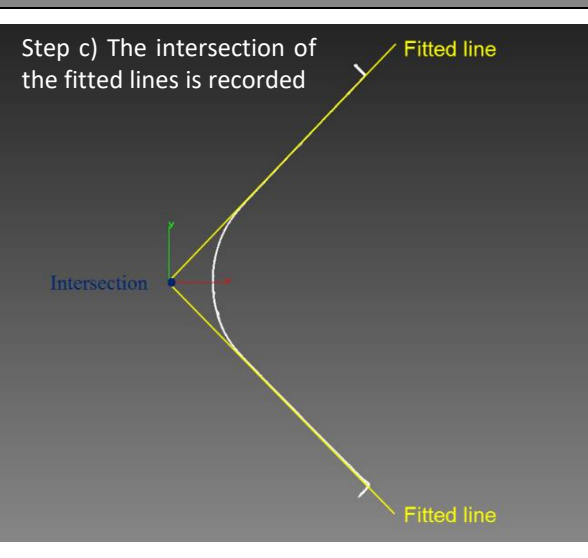
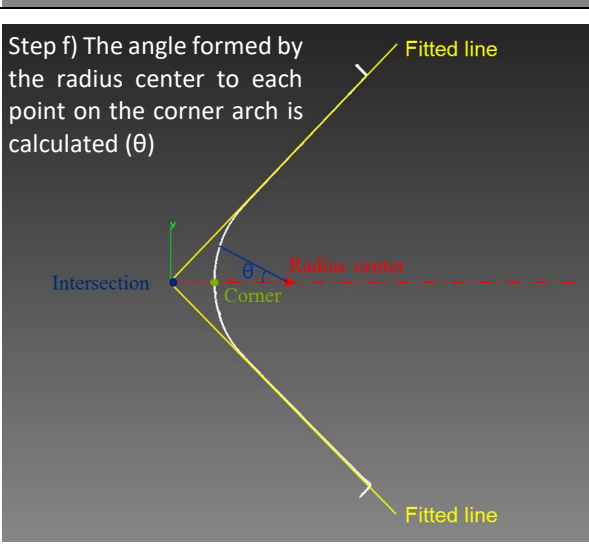
The first data point represents the angle closest to the corner. The first measurement includes points from 5 mm (buffer length) to 25 mm away from the corner. The last point represented the total spring-in, which signifies spring-in at the corner plus flange warpage effect. The total spring-in is equivalent to the traditional measurement method — fitting to the entire flanges and measure the angle from the normal vectors.

Specimens showed higher total spring-in value than corner spring-in value indicating that warpage exists in the flanges. Flange warpage is represented by the slope of the spring-in plot. The more flanges warp, the larger angle formed by vectors at increasing length (Figure 4a).

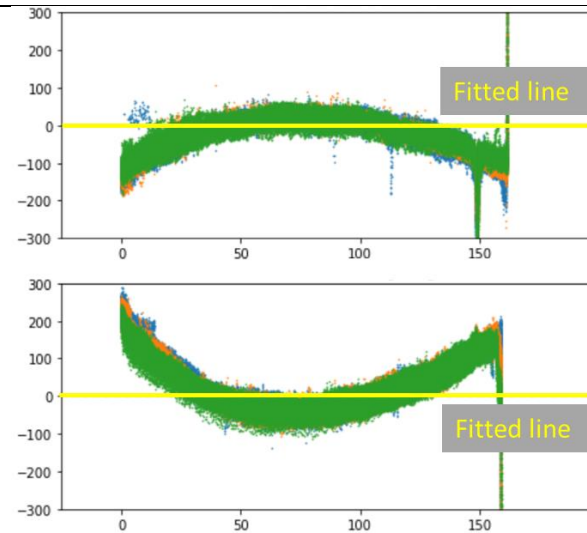
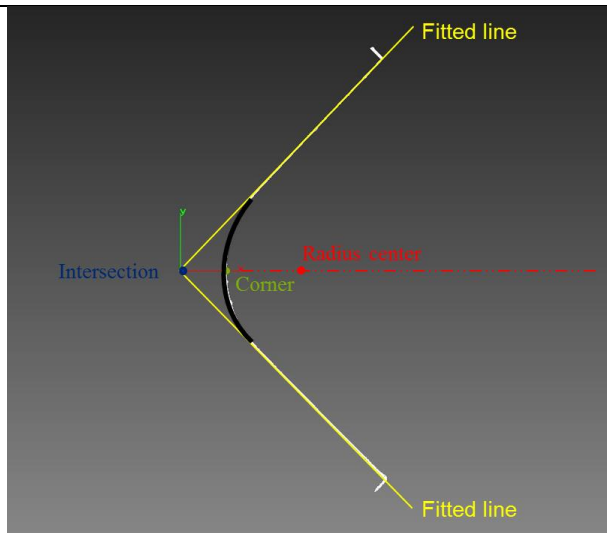
In this incremental approach, as the vector length increases, more points are being averaged, so error decreases. Conversely, the measurements are more sensitive to scatter in the point cloud closer to the corner section.

It is important to point out that the above-mentioned process is only one type of spring-in definition and representation. During the formulation of this data reduction process, it was noted that different spring-in definitions can lead to up to 0.4° difference in reported spring-in results. This is because when corner spring-in and flange warpage are combined, the resulting deformed profile is a complex curve. Thus, any spring-in angle calculated by two fitted lines or planes should be tethered to how and where the lines or planes were fitted.

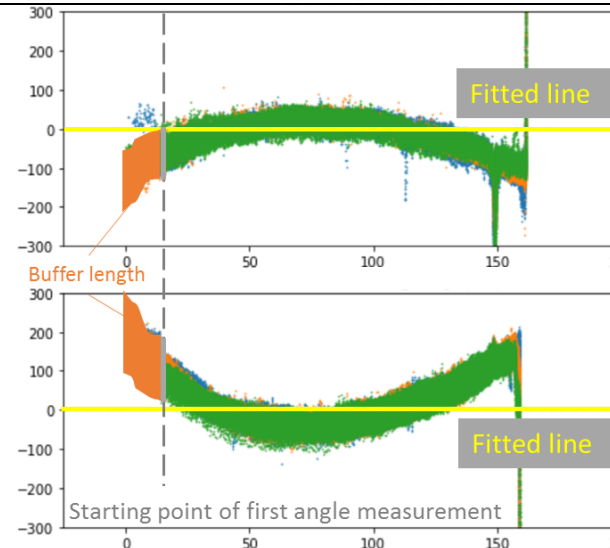
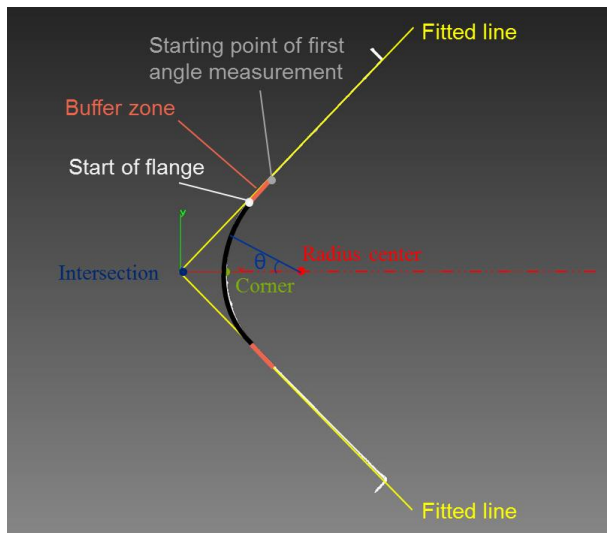
Table 1 Data reduction procedure by Python

<p>Step a) Each sectioned point cloud is analyzed in 2D</p> 	<p>Step d) The closest point to the intersection on the 2D L-profile is defined as the corner</p> 
<p>Step b) Straight lines are fitted to the flanges</p> 	<p>Step e) The point with distance R away from the corner along the vector from the intersection to the corner is defined as the radius center</p> 
<p>Step c) The intersection of the fitted lines is recorded</p> 	<p>Step f) The angle formed by the radius center to each point on the corner arch is calculated (θ)</p> 

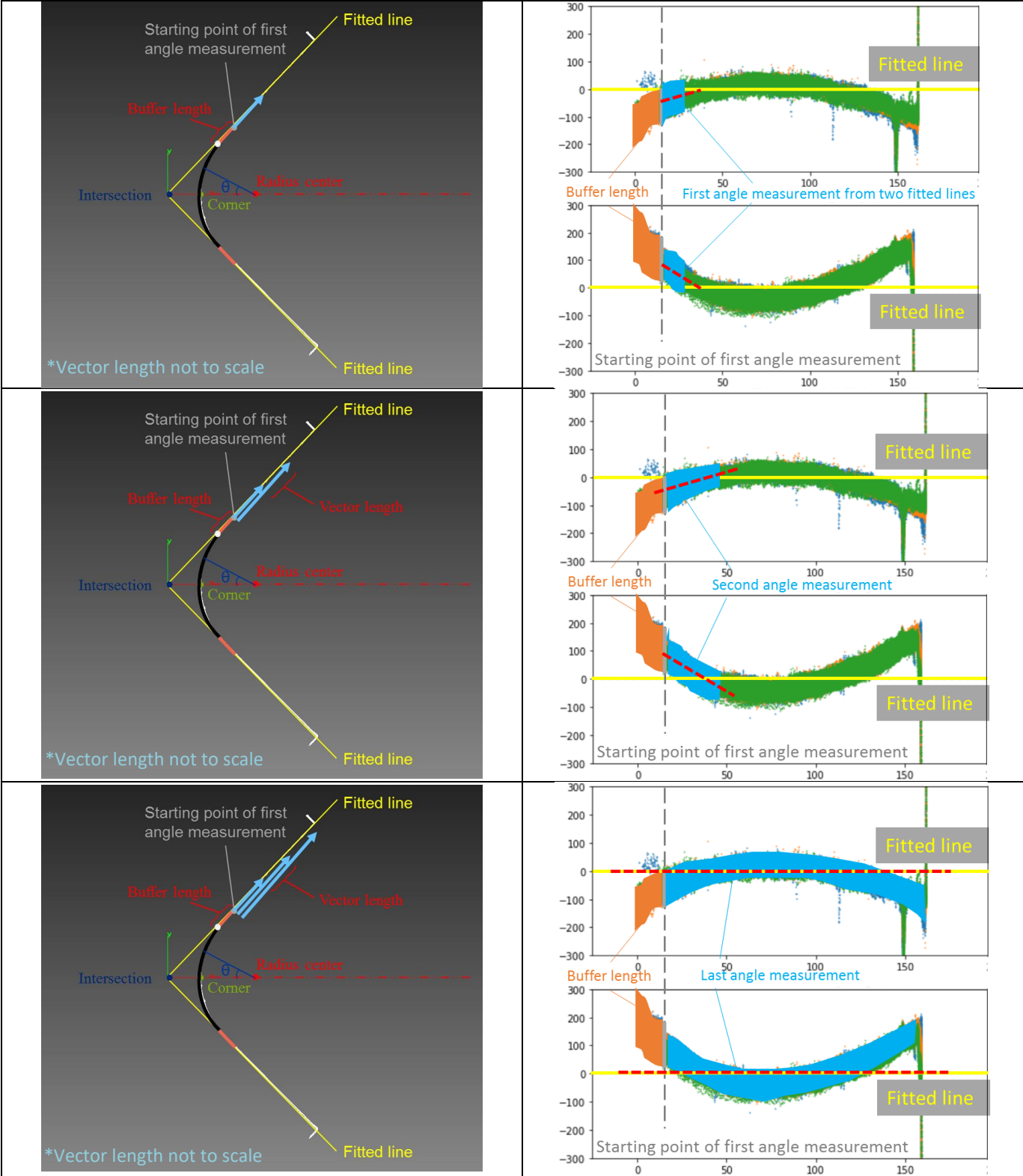
Step g) Angles within half the theoretical enclosed angle ($93^\circ/2 = 46.5^\circ$) are defined as the corner (highlighted in black). The rest are defined as the flange



Step h) A buffer zone is defined as: the end of the corner arc to where the first angle measurement starts; aimed to make sure the angle measurements do not include any corner arc. The default buffer length = 5 mm



Step i) Vectors with increasing length are fitted to each flange section with the same starting point. Then the enclosed angles of vector pairs are computed. Default increment = 5 mm



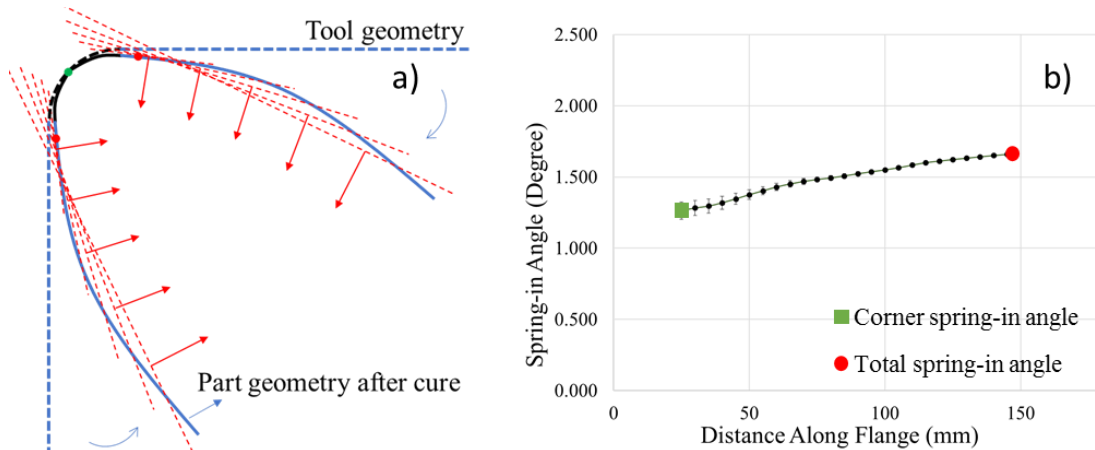


Figure 4 a) Spring-in measurement schematic in 2D. Red dots marks the end of the buffer length. Angle increase along the flange due to warpage b) A typical python script output, spring-in plot

The same data reduction approach can be used to analyze the tooling itself. This shows that within a span of 80 mm away from the corner, a tool that conforms to industrial standards will show angles that can vary from 93.06° to 93.33° (Figure 5). The angle variation is observed along the 0° direction at each location, as well as from location to location. The average variation, around 0.15° , agrees well with the observations during the initial inspection. As the measuring distance increases, the tool angle average converges to the nominal 93° . This true tool surface data should be subtracted from the uncompensated spring-in plot to provide the true L-shape deformation. Failure to do so may introduce significant error in reported spring-in angles.

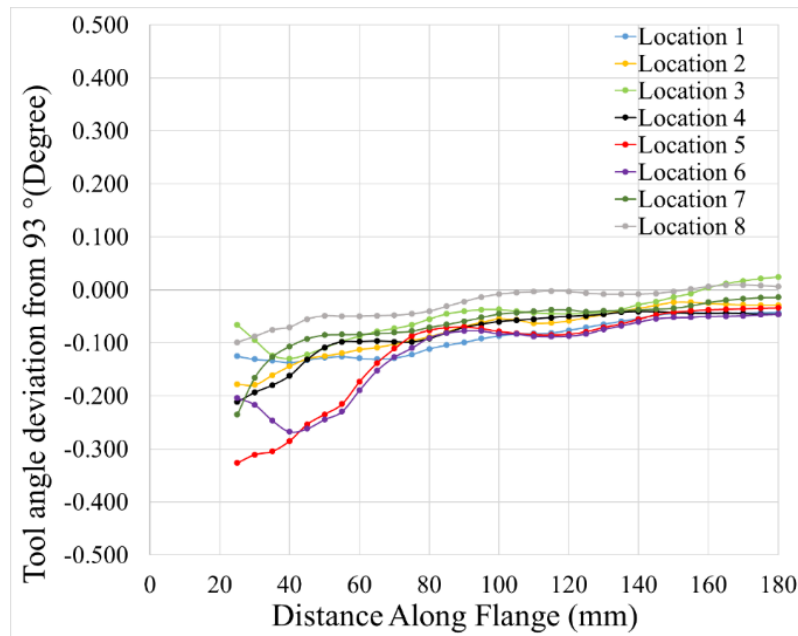


Figure 5 Tool angle deviation from nominal vs distance along the flange at specimen locations

4 Data Reporting

Based on a comprehensive review of the literature (see [1]) a list of recommended reporting items has been developed, as seen in Table 2.

Table 2 Recommended reporting items for experimental results of process induced deformation of fiber reinforced composites

		Item No.	Checklist item
Material	Material	1	Report fiber material and matrix materials and their age. Resin percentage and distribution, areal weight
	Thermal history	2	Temperature, vacuum and pressure cycles, including ramp rates and hold times experienced by specimen
	Degree of cure	3	Final degree of cure of the specimens
	Tg	4	Final glass transition temperature of the specimens
	Cure ply thickness	5	Final cure ply thickness of the specimens
	Wrinkles	6	Size, quantity and location of any wrinkles if they exist
	Bleeding	7	Resin loss during thermal transformation
	Vf	8	Final fiber volume fraction of the specimens
	Post processing	9	Report any procedures that could potentially alter specimens internal stress state, such as demolding, trimming, moisture exposure or post curing
Shape	Geometry	10	C or L or flat. Width, flange length, thickness, corner radius, corner angle, web length (applicable to C-shapes)
	Layup	11	Describe specimen layup sequence
	Ply drop off	12	Report ply drop off or other special layup techniques
	Core	13	Indicate the use of core and core materials
Tooling & consumables	Surface profile	14	Report tool surface profile, measurement method tolerance, surface roughness and deviations from nominal specification if exist. The measurement method and tolerance ideally should be the same as the specimen measurement
	Material	15	Specify the tooling material and its properties (e.g. CTE)
	geometry	16	Describe whether the tool is convex (male), concave (female) or double sided
	Sub-structure	17	State whether the tool has sub-structures and describe their effects on produced specimens
	Processing surface	18	Indicate the surface on which the specimens were processed (e.g. release agent or release film and their types)
Equipment	Equipment	19	Specify the equipment used for processing (e.g. autoclave)
	HTC	20	Heat transfer coefficient experienced by specimens during thermal transformation
Process	Manufacturing process	21	Report possible variabilities related to the manufacturing process (e.g draping and forming of the pre-preg causes fiber misalignment)
Results	Results	22	Report spring-in angles, flange warpage, number of repeats and standard deviation etc. Raw point cloud if available

5 Summary and Conclusions

This work facilitates a standardized measurement and data reduction procedure for experimentally studying process induced deformation with L-shape specimens. A robust data reduction method has been developed to accurately define and represent local L-shape deformation. This representation allows clearer linkage between manufacturing outcomes and various processing parameters. The results are also compatible with those in the existing literature and potentially with process simulations. A list of recommended reporting items to aid in the cross-comparison of L-shape data in literature has been provided. It is shown that tooling shape evaluation and L-shape deformation definition, typically overlooked by previous studies, can each affect the results by up to 0.3 ° and 0.4 ° respectively.

6 REFERENCES

- [1] Y. Tao, "Process induced deformation of composite materials: an experimental methodology, systematic review and meta-analysis," The University of British Columbia, 2021.
- [2] D. W. Radford, "Volume fraction gradient induced warpage in curved composite plates," *Compos. Eng.*, vol. 5, no. 7, pp. 923–934, Jan. 1995.
- [3] E. Kappel, "Forced-interaction and spring-in – Relevant initiators of process-induced distortions in composite manufacturing," *Compos. Struct.*, vol. 140, pp. 217–229, Apr. 2016.
- [4] C. Bellini, L. Sorrentino, W. Polini, and A. Corrado, "Spring-in analysis of CFRP thin laminates: numerical and experimental results," *Compos. Struct.*, vol. 173, pp. 17–24, Aug. 2017.
- [5] C. Bellini and L. Sorrentino, "Analysis of cure induced deformation of CFRP U-shaped laminates," *Compos. Struct.*, vol. 197, pp. 1–9, Aug. 2018.
- [6] G. Y. Fortin and G. Fernlund, "Effect of tool temperature on dimensional fidelity and strength of thermoformed polyetheretherketone composites," *Polym. Compos.*, vol. 40, no. 11, pp. 4376–4389, 2019.
- [7] K. F. Çiçek, M. Erdal, and A. Kayran, "Experimental and numerical study of process-induced total spring-in of corner-shaped composite parts," *J. Compos. Mater.*, vol. 51, no. 16, pp. 2347–2361, 2017.
- [8] C. Albert and G. Fernlund, "Spring-in and warpage of angled composite laminates," *Compos. Sci. Technol.*, vol. 62, no. 14, pp. 1895–1912, 2002.
- [9] A. Arafath *et al.*, "CCMRD 9.2 Dimensional Control for Large Complex Aerospace Structures Phase 2. Final Report," 2015.
- [10] J. Park, N. Zobeiry, and A. Poursartip, "Tooling materials and their effect on surface thermal gradients," *Int. SAMPE Tech. Conf.*, no. March, pp. 2554–2568, 2017.
- [11] Y. Tao, "Boeing - personal communication." 2020.